Plant Physiology and Biochemistry 65 (2013) 81–88

Contents lists available at SciVerse ScienceDirect

Plant Physiology and Biochemistry

journal homepage: www.elsevier.com/locate/plaphy

Research article

Effect of vulculic acid produced by *Nimbya alternantherae* on the photosynthetic apparatus of *Alternanthera philoxeroides*

Meimei Xiang [a], Shiguo Chen [b,*,1], Lianshui Wang [a], Zhangyong Dong [a], Jianghua Huang [a], Yunxia Zhang [a], Reto Jörg Strasser [b,c]

[a] Institute of Plant Pathology, Zhongkai University of Agriculture and Engineering, Guangzhou 510225, China
[b] Weed Research Laboratory, Nanjing Agricultural University, Nanjing 210095, PR. China
[c] Bioenergetics Laboratory, University of Geneva, CH-1254 Jussy/Geneva, Switzerland

ARTICLE INFO

Article history:
Received 29 October 2012
Accepted 15 January 2013
Available online 6 February 2013

Keywords:
Nimbya alternantherae
Alternanthera philoxeroides
Photosynthetic apparatus
Phytotoxin
Action site
JIP-test

ABSTRACT

The effect of the toxin vulculic acid produced by *Nimbya alternantherae*, on the photosynthetic apparatus of *Alternanthera philoxeroides*, was investigated via the photochemical activity and SDS-PAGE of protein on thylakoid membranes, fast chlorophyll *a* fluorescence transient measurements and the JIP-test. The electron transport rate of photosystem II (PSII), non-cyclic photophosphorylation activity, as well as the activity of chloroplast ATPase and Rubisco reduced significantly after vulculic acid treatment. Vulculic acid affected the O–J–I–P fluorescence induction kinetics, showing an increase of the parameters F_V/F_O, V_K and V_J and a decrease of F_O, F_M, PI_{ABS}, φ_{Po}, ψ_{Eo}, φ_{Eo}, φ_{Ro}, δ_{Ro} and PI_{total}. In addition, it significantly decreased the amounts of major photosystem I (PSI) and PSII proteins. It is concluded that vulculic acid is a photosynthetic inhibitor with multiple action sites. The main targets are the light harvesting complex (LHC) and the oxygen evolving complex (OEC) on the PSII donor side. Vulculic acid blocks electron transport beyond Q_A and on the PSI acceptor side by digesting major PSI and PSII proteins.

1. Introduction

Alligator weed (*Alternanthera philoxeroides*) is a noxious weed with worldwide distribution and a major invader of both aquatic and terrestrial habitats in China. *Nimbya alternantherae* is a pathogenic fungus causing foliar and stem necrosis of Alligator weed [1]. The fungus is a potential biological control agent since it can rapidly cause leaf-drop of the weed [1,2], and its filtrates inhibit the radicle growth of sorghum [3], attributed to a phytotoxin, 2-acetyl-3,4-dihydroxy-5-methoxyphenyl-acetic acid (vulculic acid, Fig. 1) [4]. Vulculic acid was isolated first from the metabolites of *Penicillium* sp., and showed inhibition activity to the pollen germination of black pine (*Pinus thunbergii*) with growth inhibition up to 85% at10 μg mL^{-1} [5]. The toxin (50–100 μg mL^{-1}) is non-host-specific and can quickly kill the seedlings of Alligator weed [6]. However, the mode of action of vulculic acid still remains unknown.

The previous investigations showed that vulculic acid increased cell membrane permeability and enhanced lipid peroxidation [7], and induced digestion of chloroplast membrane and distortion of chloroplast lamellae in the leaf tissue of Alligator weed [8]. We also found that the net photosynthetic rate, stomatal conductance and transpiration rate of Alligator weed leaf decrease after toxin treatment (data not published). Data suggest that vulculic acid is a photosynthetic inhibitor.

Photosynthesis, i.e. light-dependent reactions and light-independent reactions are studied by two phases. The light is catalyzed in thylakoid membranes, where the electron transport chain and H^+-ATPase are imbibed for electron flow and ATP formation. The thylakoid membrane contains four major polypeptide complexes. The PSII complex consists of a reaction center, the antenna chlorophyll proteins. PSI complex contains a reaction center and its antenna chlorophyll proteins. The intersystem electron transport is catalyzed by Cyt_b6f and connected with two mobile electron carriers (PQ and Plastocyanin) and CF_o–CF_1 complex. Photosynthesis is initiated by the absorption of light energy by the chlorophylls of both photosystems (PSI and PSII). Excitation energy is then transferred to the reaction centers P_{680} in PSII and P_{700} in PSI. P_{680} and

Abbreviations: PSII, photosystem II; PSI, photosystem I; LHC, light harvesting complex; OEC, oxygen evolving complex; PQ, plastoquinone; PC, plastocyanin; FNR, ferredoxin $NADP^+$ reductase; RuBP, ribulose-1,5-bisphosphate; LHCII, light harvesting Chl *a*/*b*–protein complex; LHCII*, LHCII trimer; RuBisCo, ribulose-1,5-bisphosphate carboxylase oxygenase; DCMU, 3-(3,4-dichlorophenyl)-1,1-dimethylurea; EDTA, ethylene diamine-tetraacetic acid; BSA, bovine serum albumin.

* Corresponding author. Tel./fax: +86 25 84395117.
E-mail addresses: chenshg@njau.edu.cn, sc768@cornell.edu (S. Chen).
[1] Present address: Boyce Thompson Institute for Plant Research, Ithaca, NY 14853, USA. Tel.: +1 607 220 9491.

0981-9428/$ – see front matter © 2013 Elsevier Masson SAS. All rights reserved.
http://dx.doi.org/10.1016/j.plaphy.2013.01.013

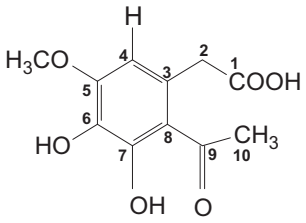

Fig. 1. The structure of vulculic acid. The molecular formula is $C_{11}H_{12}O_6$ with molecular weight of 240 g mol^{-1}.

P_{700} occur as P_{680}^{+} and $Pheo^{-}$ in PSII, and P_{700}^{+} and A_0 and FeB in PSI. And electron flow and proton translocation reactions, water splitting enzyme donates electrons to the chain and yields protons and molecular oxygen. From $Pheo^{-}$, the electron is transported to the first stable quinone electron acceptor Q_A and then to the second electron acceptor Q_B, further to the plastoquinone pool (PQ) [9]. From PQH_2, electrons are transferred via the cytochrome b6/f complex (Cyt_b6f) to plastocyanin (PC). During this reaction two protons from the PQH_2 are liberated into the internal space of the thylakoid. PC is the primary electron donor to P_{700}^{+}. From FeS^{-} the electron is transferred to soluble ferredoxin, and via ferredoxin $NADP^{+}$ reductase (FNR) to $NADP^{+}$. The protons which have been accumulated in lumen side flow back to the stroma through the H^{+}-ATPase, which phosphorylates ADP to ATP [10]. In the light-independent reactions occur carbon fixation, after and regeneration of reduction reactions, and ribulose-1,5-bisphosphate (RuBP). Photosynthesis is targeted with different inhibitors at various levels of the process [11–13].

To clarify the mechanism and localize the targets of action of vulculic acid, in this study, the effect of vulculic acid on the photosystem of Alligator weed was investigated via the analysis of photochemical activity, SDS-PAGE of protein on thylakoid membranes, fast chlorophyll *a* fluorescence transients measurements and the JIP-test.

2. Results

2.1. Effect of toxin on electron transfer reaction of thylakoid membrane

By using different electron transfer inhibitors, electron donors and electron acceptors, the PSI and PSII electron transfer activity was assessed. The PSI electron transfer rate of toxin-treated thylakoid membranes of Alligator weed was not significantly lower than that of the control except at the highest concentration, 0.208 mM, the rate of PSI electron transport decreased 16% (Fig. 2). However, at the same concentration of toxin the electron transfer rate of PSII lowered by 48% (Fig. 2).

2.2. Effect of toxin on photophosphorylation and ATPase activity

Thylakoid membranes were kept in ice-bath for 30 min, the cyclic or non-cyclic photophosphorylation rate was measured with and without toxin. The results show that the cyclic photophosphorylation rate was not significantly lower than control except at 0.208 mM the rate decreased by 7.5% (Fig. 3). However, the non-cyclic photophosphorylation rate lowered by 42%, at 0.208 mM toxin (Fig. 3).

On the other hand, both Mg^{2+}-ATP and Ca^{2+}-ATP activities of toxin-treated thylakoid membranes of Alligator weed were significantly lower than that of the control. The activity of Mg^{2+}-ATPase and Ca^{2+}-ATPase decreased by 41% and 39%, respectively, at the highest concentration (0.208 mM of toxin) (Fig. 4).

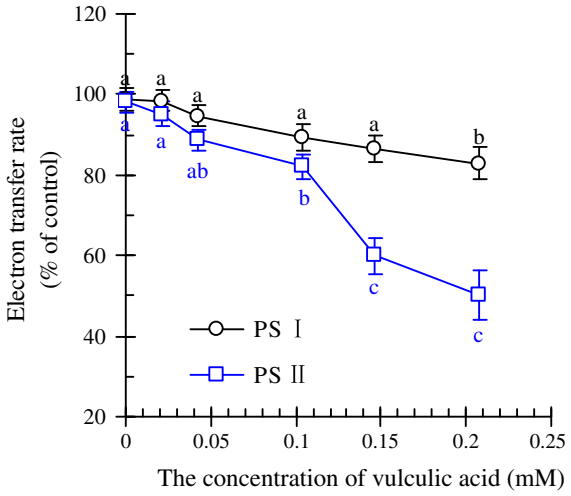

Fig. 2. The electron transfer rate of Alligator weed chloroplasts after treatment with different concentration of vulculic acid. The electron transfer rate was determined after the samples were treated for 30 min. Data are mean values ± SE. PSI and PSII electron transfer rate of control is 191.85 ± 5.45, 19.98 ± 0.56 μmol O^2 mg^{-1} Chl h^{-1} (100%), respectively. Different letters indicate values significantly different between treatments ($P < 0.05$) according to Duncan's multiple range test (SSR).

2.3. Effect of toxin on the content of thylakoid membrane protein

The results show that there are no remarkable differences between the treatments of 0.021, 0.042, 0.104 mM toxin compared with control in the thylakoid polypeptides. However, the contents of major PSI and PSII proteins, including PSI core peptide PsaA/PsaB, PSII core antenna chlorophyll-binding protein (CP43, CP47, CP29, CP26 and CP24), light harvesting Chl *a*/*b*–protein complex (LHCII) and OEC 33 kD, decreased significantly at 0.146 mM toxin (Fig. 5). The bands near 66 kD disappeared, therefore PSII core peptide LHCII trimer (LHCII*) and D1/D2 dimer were the polypeptides degraded. The result indicates that the toxin can lead the digestion of membrane proteins, especially PSII proteins.

2.4. Effect of toxin on activity of RuBisCo

The results show that both enzymes RuBP carboxylase and oxygenase activities of toxin-treated extract of Alligator weed are

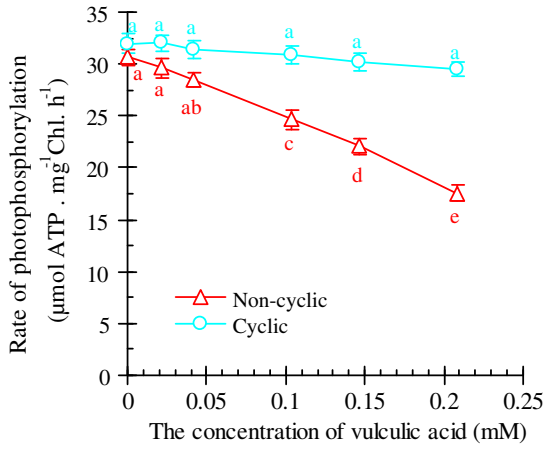

Fig. 3. The photophosphorylation rate of Alligator weed chloroplasts after treatment with different concentrations of vulculic acid. The photophosphorylation rate was determined after the samples were treated for 30 min. Data are mean values ± SE. Different letters indicate values significantly different between treatments ($P < 0.05$) according to Duncan's multiple range test (SSR).

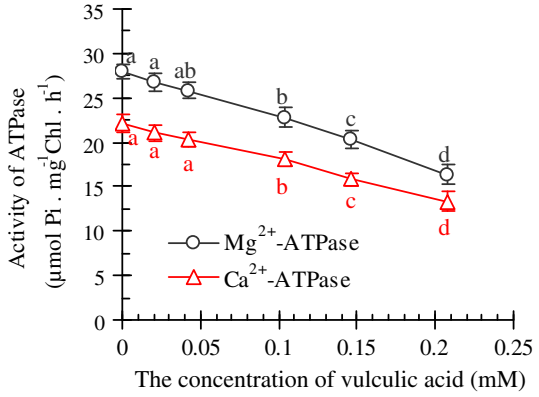

Fig. 4. ATPase activity of Alligator weed chloroplasts after treatment with different concentrations of vulculic acid. Data are mean values ± SE. Different letters indicate values significantly different between treatments ($P < 0.05$) according to Duncan's multiple range test (SSR).

lower than control (Fig. 6). The RuBP carboxylase activity declined by 31.6% at 0.208 mM toxin treatment (Fig. 6A). The RuBP oxygenase activity also decreased by 36%by the same toxin concentration (Fig. 6B).

2.5. Effect of toxin on fast Chl a fluorescence induction transient OJIP curves

To search for the precise action site of vulculic acid in PSII, fast Chl *a* fluorescence rise transients OJIP [14,15]of leaf discs of *A. philoxeroides* treated with the toxin were determined. Fig. 7 shows fluorescence transient curves of control, toxin- and DCMU (3-(3,4-dichlorophenyl)-1,1-dimethyl-urea)-treated leaves. The toxin- and DCMU-treated leaves exhibited different transient curves compared to control. At 2 ms the 'J' step, the fluorescence intensity of DCMU-treated leaves was significantly higher than the toxin-treated leaves and control (Fig. 7A and B). With increasing treatment time of toxin exposure, the J step moved to the P level. At 0.5 mM vulculic acid treatment for 48 h, the F_J was so closer to the F_M maximum value that the OJ phase had become the main part of the OJIP transient and the step-I disappeared. With increasing incubation time, the relative variable fluorescence at the J-step, V_J, increased by 10% (6 h), 22% (12 h), 45% (24 h), 55% (36 h) and 64% (48 h) as compared with the control (as 100%, $V_J = 0.51$). The initial relative slope of the fluorescence rise from F_O to F_J showed a time-dependent rise, suggesting that the toxin blocked electron

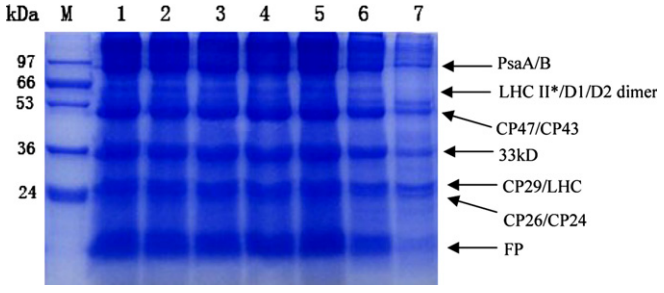

Fig. 5. SDS-PAGE analyses of thylakoid membrane protein from Alligator weed after treatment with vulculic acid for 30 min. Seeing from left to right, M and 1–7, represents different treatment: marker (M); control (1); ddH_2O (2); phosphate buffer (3); 0.021 mM (4), 0.042 mM (5), 0.104 mM (6) and 0.146 mM (7) toxin. PsaA/PsaB indicate PSI core peptide; CP43, CP47, CP29, CP26 and CP24 indicate PSII core antenna chlorophyll-binding protein; LHCII, 33 kD; LHCII* and D1/D2 indicate light harvesting Chl a/b–protein complex, oxygen evolving complex 33 kD, LHCII trimer and D1/D2 dimer, respectively; FP indicate carotenoid.

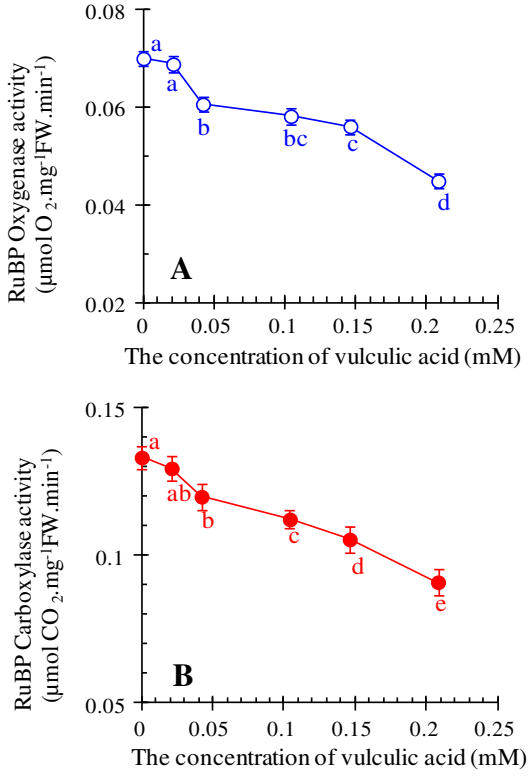

Fig. 6. RuBisCo activity of Alligator weed leaves after treatment with different concentrations of vulculic acid. (A) RuBP carboxylase activity; (B) RuBP oxygenase activity. Data are mean values ± SE. Different letters indicate values significantly different between treatments ($P < 0.01$) according to Duncan's multiple range test (SSR).

transport rate from Q_A to Q_B resulting in Q_A^- accumulation. The 'thermal phase' (J–I–P) of the fluorescence rise showed no significant difference among different treatments, due to closure of PSII reaction centers at high light intensity [16].

The difference kinetics $W_{OJ} = (F_t - F_O)/(F_J - F_O)$ was also plotted in the 0–2 ms time range. Significant change in the amplitude of the K-band (at 300 μs) was observed with 0.5 mM toxin (Fig. 7C), the result indicates that vulculic acid interacted and inhibited at OEC level. This hypothesis was further supported by appearance of K-step, and V_K, increased by 18% (6 h), 29% (12 h), 68% (24 h), 79% (36 h) and 79% (48 h) as compared with the control ($V_K = 0.28$). In Fig. 7D, the relative variable fluorescence $W_{OI} = (F_t - F_O)/(F_I - F_O)(W_{OI} > 1)$ is presented in a linear time scale from 30 ms (I-step) to 330 ms (P-step), which corresponds to the reductions of PSI to $NADP^+$. The effects of the toxin on W_{OI} value showed a time-dependent decrease. These results indicate that vulculic acid has a distinct effect on electron flow at the PSI acceptor side.

2.6. JIP-test

Each OJIP transient can be analyzed according to the equations of JIP-test [14]. In the radar plot (Fig. 8), the maximum yield of primary photochemistry ($\varphi_{Po} = TR_0/ABS$) values had no significant difference up to 12 h incubation of toxin as compared with DCMU and water treatment. But by further increasing the incubation time, the φ_{Po} of the toxin treatment decreased. In contrast to φ_{Po}, the probability that a trapped exciton moves an electron into the electron transport chain beyond Q_A ($\psi_{Eo} = ET_0/TR_0$), as well as the quantum yield for electron transport ($\varphi_{Eo} = \varphi_{Po} \cdot \psi_{Eo}$) decreased strongly as a function of the incubation time with 0.5 mM toxin.

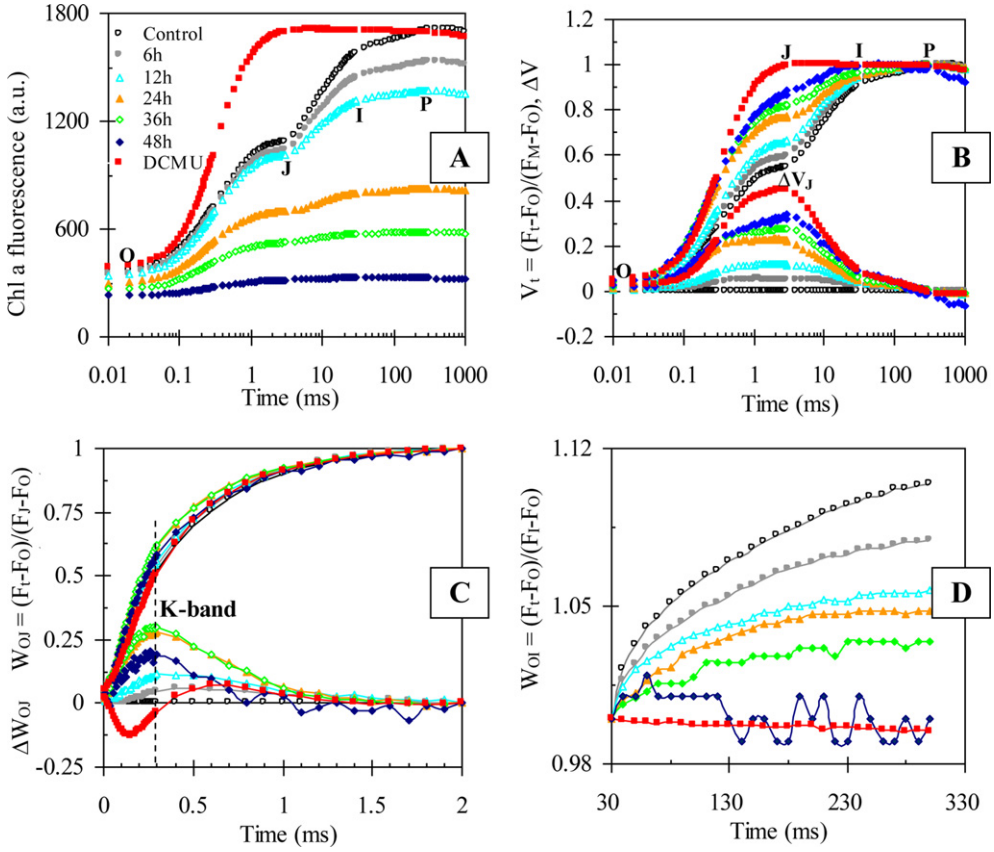

Fig. 7. Chlorophyll fluorescence rise kinetics of Alligator weed leves after treatment with vulculic acid. OJIP curves of leaf discs incubated under dark with 0.5 mM toxin solution or 0.2 mM DCMU or distilled water at room temperature for indicated times were detected using Handy PEA. (A) Relative variable fluorescence (V) from raw data; (B) relative variable fluorescence between F_O and F_M: $V_t = (F_t - F_O)/(F_M - F_O)$ (the top figures); $\Delta V_t = \Delta(F_t - F_O)/(F_M - F_O)$ (the bottom figures); (C) relative variable fluorescence between F_O and F_J: $W_{OJ} = (F_t - F_O)/(F_J - F_O)$; (D) relative variable fluorescence between F_O and F_I: $W_{OI} = (F_t - F_O)/(F_I - F_O)$.

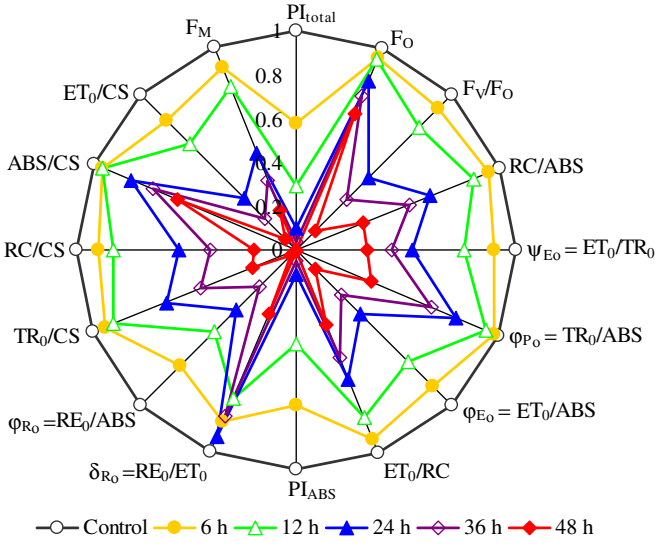

Fig. 8. Radar plot presentation of some parameters quantifying PSII behavior derived from JIP-test. The leaf discs of Alligator weed were incubated for indicated times with 0.5 mM of vulculic acid and 0.2 mM DCMU. Each parameter is expressed as fraction relatively to the values of the control (regular circle with value 100% = 1). Data were obtained from the data table of the OJIP traces shown in Fig. 7A, B.

These results indicate that the toxin inhibited the primary light reaction and the redox reactions after Q_A due to interruption of electron flow from Q_A^- toward PSI.

The performance index PI_{ABS} is used to quantify the PSII behavior. It's clear that the average of PI_{ABS} declined sharply by further increasing the time of treatment (Fig. 8). When leaves were incubated with toxin for 48 h, PI_{ABS} decreased to around 0.8% than control, almost the same as a DCMU-treated leaf. This indicates that the most important determinant of the loss of PSII structure and function is the decline of quantum yield for PSII electron transport due to blockage of electron transfer beyond Q_A.

The performance index, PI_{total}, measuring the performance upto the reduction of PSI end electron acceptors (RE), is the most sensitive parameter of the JIP-test because it incorporates several electron transport steps: $\varphi_{Po} = TR_0/ABS$, $\psi_{Eo} = ET_0/TR_0$, $\gamma_{RC} = Chl_{RC}/Chl_{total}$ and $\delta_{Ro} = RE_0/ET_0$. The PI_{total} decreased by 99.8% (Fig. 8). Moreover, the quantum yield for reduction of end electron acceptors at the PSI acceptor side (φ_{Ro}) and the probability that an electron is transported from the reduced intersystem electron acceptors to final electron acceptors of PSI (δ_{Ro}) decreased greatly, indicating that the toxin has interacting effect at the PSI acceptor side. The toxin treatment had an effect on the IP phase (Fig. 7D), which is related to electron transfer through PSI and the reduction of a traffic jam of electrons caused by a transient block at the acceptor side of PSI due to the inactivation of FNR [17].

The initial fluorescence F_O when all RCs were open decreased by 32% up to48 h treatment in 0.5 mM toxin. However, the maximal fluorescence intensity F_M value, declined by 80% at the same incubation time and toxin concentration (Fig. 8). The results indicate

that the toxin affected the structure and function of the LHC of PSII. Moreover, the ratio of F_V/F_O reduced by 88% at 48 h of toxin incubation. It indicates that active Q_A reducing RCs were converted into non-Q_A reducing heat sink centers.

3. Discussion

Vulculic acid is a polyketide, which has been found to inhibit pollen germination of black pine [5]and affect the chloroplast ultrastructure of Alligator weed [8]. Like tenuazonic acid [11,12] and the tetramic acid derivative 3-AIPTA [13], here vulculic acid is also a PSII inhibitor since it strongly blocks PSII electron transport (Fig. 2) and non-cyclic photophosphorylation (Fig. 3). The photosynthetic electron transport is coupled to a buildup of a thylakoid proton gradient, which drives the synthesis of ATP from ADP and phosphate catalyzed by the chloroplast ATPase [18]. Vulculic acid inhibited prominently the activity of chloroplast ATPase (Fig. 4). Inhibition of ATPase activity will inevitably lead to blocking ATP synthesis and ATP-hydrolysis. Precisely because vulculic acid interrupts PSII electron flow and ATP synthesis, it is regarded as an inhibitor of redox energy and binding energy conservation.

The enzyme ribulose-1,5-bisphosphate carboxylase oxygenase (RuBisCo) is a key enzyme in light-independent reactions, involving in the first major step of carbon fixation. In toxin-treated crude enzyme extracts both carboxylase and oxygenase activities of RuBisCo were lower significantly than that of control (Fig. 6). This suggested that vulculic acid inhibited the activity of the enzyme, disrupting the tricarboxylic acid cycle or photorespiration of Alligator weed, and hence the efficiency of carbon assimilation declined.

Fast Chl *a* fluorescence induction rise reveals a characteristic OJIP polyphasic transient at room temperature when the transients are plotted on a logarithmic time scale [19]. While there-oxidation of Q_A^- is inhibited by stress (such as the presence of inhibitors), the fluorescence transient rises from O (origin point) to P (fluorescence peak) is markedly faster. During this O to J phase, mainly single-turnover events with respect to Q_A reduction are occurring [20]. With longer duration of vulculic acid treatment, a strong increase of the J level was the greatest change in fluorescence transients OJIP (Fig. 7). An increase of the J step is usually interpreted as an evidence for a large accumulation of the reduced form of Q_A (Q_A^-) due to a slowdown of electron transport beyond Q_A [19,20].

The J level is linked to the balance between efficiency and in efficiency of the light-independent reactions after Q_A^- expressed by ψ_{Eo}. Once inhibition of PSII electron flow beyond Q_A occurred, the maximum quantum yield of PSII electron transport further than Q_A^- (φ_{Eo}) would have a sharp decrease. The maximum quantum yield of primary photochemistry, φ_{Po}, reflects the efficiency of the light reactions only [15,21]. In the case of vulculic acid treatment, a sharp decline of ψ_{Eo} and φ_{Eo} and the decrease of φ_{Po} at increasing incubation time (Fig. 8) indicate that vulculic acid inhibited both the primary light reaction and the redox reaction after Q_A.

The performance index (PI_{ABS}) combines the responses due to the photochemical and nonphotochemical properties as well as due to the density of active reaction centers per chlorophyll absorption as indicated by the symbol γ_{RC} [15,22]. Vulculic acid incubation can cause an overall decrease of the PI_{ABS} values with the addition of vulculic acid-treated time (Fig. 8). PI_{ABS} is composed of three independent components, γ_{RC} (the density of RC in the chlorophyll domain), φ_{Po}, and ψ_{Eo} [15,22]. A lowering of the PI_{ABS} values can be attributed to the change of one, two, or three parameters. Vulculic acid acts on ψ_{Eo}, φ_{Po}, and γ_{RC}, but ψ_{Eo} is most sensitive (Fig. 8). We concluded that the most direct factor of the decrease of PI_{ABS} is a rapid lowering of the efficiency of the redox reaction of the electron transport chain.

With the decline in initial fluorescence F_O and maximal fluorescence intensity F_M as well as the ratio of F_V/F_O, combined with the evidence that the effect of vulculic acid on the K-band reflecting the OEC activity [15] (Fig. 7C and D), we propose that vulculic acid affects the LHC and the OEC at the PSII donor side, which is different from the classical inhibitor site of DCMU. The SDS-PAGE analysis of thylakoid membrane proteins further indicated that the toxin could lower the content of LHCII and OEC 33 kD (Fig. 5). The direct cause of the decrease of LHC and OEC function might be the digestion of the protein complexes.

Current models of the fluorescence OJIP transients show the J step as corresponding to the concentrations of $Q_A^-Q_B$ and $Q_A^-Q_B^-$ formed by electron transport from Q_A to Q_B, to I, the first shoulder in the increase in concentration of $Q_A^-Q_B^{2-}$. The "P" peak coincides with maximum concentrations of $Q_A^{2-}Q_B^{2-}$ and PQH_2 and the reduction of the acceptor side of PSI, equivalent to the process of the electron transportation from Q_B to PQ and further to PSI [23,24]. The OJ phase is largely driven by primary photochemistry, where only single-turnover Q_A reduction events are carried out. The JP phase is dominated by the biochemical reaction, where multiple-turnover Q_A reduction events are performed. The most important influence of vulculic acid is on multiple-turnover Q_A reduction events (Figs. 7 and 8). And the disappearance of D1/D2 dimer band in SDS-PAGE of the thylakoid membrane protein (Fig. 5) indicated that the mode of action of vulculic acid on D1 protein could be digestion of the protein.

The performance index, $PI_{total} = PI_{ABS} \cdot \delta_{Ro}/(1 - \delta_{Ro})$, incorporates the maximal performance for electron transport from water to PQ and PC per chlorophyll (PI_{ABS}) and the performance to reduce an end electron acceptor at the PSI acceptor side [22]. A dramatically decrease of PI_{total} not only resulted from the loss of PSII activity but also from the damage of PSI structure and function. The IP phase is related to electron transfer through PSI and the decrease of a traffic jam of electrons caused by a transient block at the acceptor side of PSI due to the inactivation of FNR [17]. A smaller *I–P* amplitude and a lower φ_{Ro} level (Figs. 7D and 8) indicate that longer incubation times in vulculic acid can cause a loss of the structure and function of PSI resulting from inhibiting electron donation and the reduction of end electron acceptors on the PSI acceptor side.

Based on the above results, it is concluded that vulculic acid is a photosystem inhibitor with several action sites, including electron transfer chain, chloroplast ATPase, and RuBisCo in light-independent reactions. The main targets of the toxin are the LHC and the OEC of PSII donor side, blocking electron transport beyond Q_A and of PSI acceptor side by digesting major PSI and PSII proteins. The formation of reactive oxygen species resulting from the inhibition of the photosystems might be the key for why the toxin destroys cell membranes leading to cell death. However, more studies are needed to elucidate the action mode of vulculic acid.

4. Materials and methods

4.1. Plant materials

The plants of Alligator weed obtained from the campus of Zhongkai University of Agriculture and Engineering in Guangzhou, China, were grown for two months by rooting in Hoagl & Arnon nutrition liquid in a greenhouse at 30/25 °C day/night temperatures, under natural illumination and approximately70% relative humidity. The fourth leaf from the top of each plant was used in bioassay.

4.2. Toxin materials

Vulculic acid was isolated and purified from the culture filtrate of *N. alternantherae* [4] by first transferring conidia from potato

dextrose agar to 200 mL modified Fries broth in 500 mL conical flasks, at 25 °C, 120 rpm for 7 d, and finally transferring mycelia to another 200 mL modified Fries broth, at 28 °C, 200 rpm for 7 d. Methanol was added into the filtrate at a volume ratio of 1/3 (methanol/filtrate, v/v), and the contents were mixed with a glass rod, filtered with Whatman #1filter paper, and the solid mater was washed with methanol 2–3 times. The filtrate was passed through a column of macroporous resin DM-130 (Shandong Lukang Pharmaceutical Group Co., Ltd., Jining, China), and the column eluted with methanol. The methanol-diluted extraction was concentrated by rotary evaporator under regular pressure at 60 °C, and the crude product was then extracted with ethyl acetate. The ethyl acetate extraction was dissolved with a mixture of benzene/acetone (1/1, v/v) at 60 °C and filtered. After crystallizing and re-crystallizing in an ice-bath for two to three times, the impure crystals were purified again by chromatography in a silicagel column, and eluted with the same mixture of benzene/acetone (1:1). The eluent was re-crystallized in the ice-bath, and finally HPLC was performed until a white needle material, the purified toxin, was obtained. The condition for HPLC was 250 mm × 4.6 mm C_{18} column, 20 μL sample size, 1 mL min^{-1} flowrate of mobile phase, 208 nm UV detection. Mobile phase was prepared by dissolving 0.58 g ethylene diamine-tetraacetic acid (EDTA), 1.18 g heptanesulfonate sodium, 25 mL acetic acid and 5 mL triethylamine in 970 mL double-distilled water, and regulating pH to 3.7 via acetic acid and triethylamine. A 1000 mL of the solution was mixed with 140 mL of methanol. The mixture then was filtered and ultra-sounded for 20 min.

4.3. Thylakoids treatment

The thylakoid was isolated using a method slightly modified from Jursinic [25]. Leaf samples were homogenized in ice-cold grinding medium containing 50 mM Tris–HCl (pH 7.6), 0.4 mM sucrose, 5 mM $MgCl_2$, 15 mM NaCl, 5 mM vitamin C and 0.05% bovine serum albumin (BSA). The homogenate was filtered through two layers of miracloth and the filtrate was centrifuged at 500 *g*, 0 °C for 2 min and then the supernatant centrifuged at 4000 *g*, 0 °C for 4 min. The chloroplast pellets were suspended in a low osmotic medium containing 50 mM Tris–HCl (pH7.6), 5 mM $MgCl_2$, 15 mM NaCl for washing and then the suspension was centrifuged at 10,000 *g*, 0 °C for 7min. The thylakoid pellets were re-suspended in a small volume of the low osmotic medium and stored in liquid nitrogen for later use. The chlorophyll concentration was analyzed as described by Arnon [26].

Toxin dissolved in double-distilled water was added to thylakoid suspensions to give final concentrations of 0.021, 0.042, 0.104, 0.146 and 0.208 mM, using double-distilled water as controls. The samples were used to analyze ATPase activity, or electron transfer rate and photophosphorylation rate after being treated in ice-bath for 30 min. The inhibitory activities were calculated as the percent inhibition compared to controls. The data were subjected to Analysis of Variance. Where significant treatment effects were found, the means were separated by Duncan's multiple range test at $p = 0.05$.

4.4. Electron transfer rate assay

Measurement of electron transfer rate of PSII and PSI electron transport chain was performed by a method slightly modified from Coombs et al. [27].

PSI reaction medium (2.0 mL) contained 50 mM Hepes–KOH buffer (7.6), 50 μM methyl viologen, 5 mM NH_4Cl, 2 mM NaN_3, 50 μM DCMU, 0.2 mM dichlorophenol–indophenol, 2 mM vitamin C and thylakoid suspensions of 50 μg chlorophyll.

PSII reaction medium (2.0 mL) contained 50 mM Hepes–KOH buffer (7.6), 4 mM $K_3Fe(CN)_6$, 5 mM NH_4Cl, 1 mM *p*-phenylenediamine and thylakoid suspensions of 50 μg chlorophyll.

Oxygen evolution was measured by a Clark type oxygen electrode (SG-6 oxygen detector, Hansatech, the U.K.) and the reaction started by illumination at 1300 μmol m^{-2} s^{-1}, 25 ± 2 °C for 5 min. The experiment was repeated three times.

4.5. Photophosphorylation activity assay

The measurement of the rate of cyclic and non-cyclic photophosphorylation was carried out by a method slightly modified from Li and Wei [28]. The reaction media contained a solution [25 mM Tris–HCl (pH7.8), 30 mM NaCl and 6 mM $MgCl_2$] 0.4 mL, 5 mM ADP–Na_2 0.2 mL, 0.06 mM phenazine methosulfate 0.2 mL (for cyclic photophosphorylation) or 1 mM $K_3[Fe(CN)_6]$ 0.2 mL (for non-cyclic photophosphorylation), 8 mM KH_2PO_4 0.2 mL, treated thylakoid suspensions of 75 μg chlorophyll and H_2O 0.2 mL. All reaction mixtures were conducted with illumination at 1300 μmol m^{-2} s^{-1}, 20 °C for 8 min. The experiment was repeated three times.

Measurement of chloroplastic ATPase activities was performed by a method slightly modified from Huang [29]. Mg^{2+}-ATPase reaction medium contained 0.25 M Tris–HCl (pH 8.0) 0.1 ml, 0.05 M $MgCl_2$ 0.1 mL, 0.5 M NaCl 0.1 mL, 0.5 mM phenazine methosulfate 0.1 mL, 0.05 M dithiothreitol 0.1 mL, H_2O 0.3 mL and treated thylakoid suspensions of 50 μg chlorophyll min in a 20 °C water-bath, and then 0.1 mL of 50 mM ATP was added and incubated. The reaction mixtures were illuminated under 1300 μmol m^{-2} s^{-1} light for at 37 °C for 5 min. Finally 0.2 mL of 20% trichloroacetic acid was added to stop the reaction. The Ca^{2+}-ATP reaction medium contained 0.25 M Tris–HCl (pH 8.0) 0.1 mL, 20 mM EDTA 0.1 mL, 10 mM ATP 0.1 mL, 0.1 M $CaCl_2$ 0.1 mL, 2 g L^{-1} trypsinase 0.1 mL, H_2O 0.3 mL and thylakoid suspensions of 50 μg chlorophyll. The reaction mixtures were kept under 1300 μmol m^{-2} s^{-1} light for 5 min, put into a 20 °C water-bath for 10 min, and 0.1 mL of 10 g L^{-1} BSA added to stop the reaction. The experiment was repeated three times.

4.6. SDS-PAGE of thylakoid membrane

After being incubated for 30 min with vulculic acid and centrifuged, peptides from thylakoid membranes were analyzed by SDS-PAGE in a system containing 6 M urea. After electrophoresis, the gels were stained with Coomassie brilliant blue.

4.7. RuBisCo treatment

A crude extraction of RuBisCo was done using a method slightly modified from Perchorowiczet al. [30]. Leaf tissue (2.5 g) was ground with 15 mL buffer [100 mM Tris–HCl (pH7.6), 2 mM EDTA, 10 mM $MgCl_2$, 10 mM $NaHCO_3$, 10 mM mercaptoethanol, 2% polyvinylpyrrolidone] in a glass mortar maintained at 0–4 °C. The homogenate was filtered through two layers of miracloth and the filtrate was centrifuged at 15,000 *g* for 30 min at 4 °C. The protein contents of samples were determined as described by Bradford [31].

Toxin dissolved in double-distilled water was added to the rough enzyme extracts to give final concentrations of 0.021, 0.042, 0.104, 0.146 and 0.208 mM using double-distilled water as controls with three repetitions per treatment. The samples were analyzed for RuBisCo activity after mixing.

4.8. RuBisCo activity assay

The activity of RuBP carboxylase was measured via a method slightly modified from Perchorowiczet al. [30]. The assay mixture

contained a reagent [100 mM Tris–HCl (pH 8.0), 10 mM $MgCl_2$, 5 mM ATP, 5 mM dithiothreitol, 0.2 mM NADH and 0.1 mM EDTA] 1.7 mL, H_2O 1.0 mL, 10 mM $NaHCO_3$ 0.1 mL, 5 U glyceraldehydes-3-phosphate dehydrogenase/3-phosphoglyceratekinase 0.1 mL, and treated crude enzyme extract 0.1 mL (0.4 mg protein). After attaining full activation at 30 °C for 10 min and measuring OD_1 at 340 nm, 1 mL 0.3 mM RuBP was added to start the reaction. The reaction was stopped after 45 s by addition of 0.1 mL 4 M HCl, and OD_0 at 340 nm was measured. The inhibitory activities were calculated as the percent inhibition compared to controls. The data were subjected to Analysis of Variance. Where significant treatment effects were found, the means were separated by Duncan's multiple range test at $p = 0.05$.

For the activity of RuBP oxygenase, the assay mixture was in saturation of the air and contained a solution [100 mM Tris–HCl (pH8.0), 20 mM $MgCl_2$, 0.4 mM EDTA and 5 mM dithiothreitol] 2 mL and treated rough enzyme extracts 0.1 mL (0.4 mg protein). After incubation at 25 °C for 10 min and measuring oxygen consumption per minute (V_1) by SG-6 oxygen detector, 0.1 mL of 0.3 mM RuBP was added to start the reaction and the variation of oxygen consumption per minute (V_0) was measured.

4.9. Measurements of fast chlorophyll a fluorescence transients and the JIP-test

In recent years, fast Chl *a* fluorescence transients OJIP have become a useful tool to investigate the conditions of the structure, conformation and function of the overall photosynthetic apparatus. On a logarithmic time scale, the course of chlorophyll fluorescence induction from F_O to F_M under continuous illumination was divided into three phases by four points, which were 'O' (0 ms, origin point), 'J' (2 ms), 'I' (30 ms), and 'P' (200–500 ms), respectively [14,15].

Whole plants of *A. philoxeroides* were dark-adapted for at least 1 h before the treatments. Subsequently, leaf discs of 9-mm diameter were prepared and rinsed with distilled water, and then submerged in a 0.5 mM toxin solution or 0.2 mM DCMU or distilled water in complete darkness at room temperature. Chl *a* fluorescence transient OJIP curves were measured at room temperature with a plant efficiency analyzer (Handy PEA fluorometer, Hansatech Instruments Ltd., King's Lynn, UK) as described by Strasser and Govindjee [19]. Chl fluorescence was induced by 1 s pulses of red light (650 nm, 3500 μmol m^{-2} s^{-1}). The same experiment was repeated at least 10 times. Raw fluorescence OJIP transients were transferred with Handy PEA V1.30 software and BiolyzerHP3 to a spreadsheet. The data were then analyzed using equations of the JIP-test parameters. The JIP-test defines the maximal (subscript "O") energy fluxes in the energy cascade for the events absorption (ABS), trapping (TR_0), electron transport (ET_0) and reduction of end-electron acceptor of PSI (RE_0). EC is a pod of the reducible electron carriers. In this paper the following original data were utilized: initial fluorescence F_O was measured at 20 μs since, at this time, all reaction centers (RCs) are open; fluorescence intensity at 300 μs (K-step) was denoted as $F_{300\mu s}$; fluorescence intensity F_J was at 2 ms (J-step); fluorescence intensity F_I was at 30 ms (I-step); maximal fluorescence intensity F_M is equal to F_P since the pulse was saturating. The 'O to J' phase reflects the partial reduction and reoxidation of the quinone electron acceptor Q_A in PSII. The higher the 'J' step implies that electron transfer from Q_A to Q_B (secondary quinine electron acceptor) is blocked [19]. PSII behavior was characterized on the basis of several parameters derived from the OJIP-transients using the following formulas [15]:

The relative variable fluorescence at J step denoted as V_J, reflecting the fraction of Q_A^-/Q_{Atotal}:

$$V_J = (F_J - F_O)/(F_M - F_O)$$

The relative variable fluorescence at K step denoted as V_K:

$$V_K = (F_K - F_O)/(F_M - F_O)$$

The flux ratios, probabilities or yields, for example the probability ψ_{Eo} that a trapped exciton moves an electron into the electron transport chain beyond Q_A^- is given as:

$$\psi_{Eo} = ET_0/TR_0 = 1 - V_J$$

The maximum quantum yield of primary photochemistry, φ_{Po}, was defined as according to the general equation to express the quantum yield of primary photochemistry:

$$\varphi_{Po} = TR_0/ABS = 1 - F_O/F_M$$

The maximum quantum yield of electron transport (φ_{Eo}) between PSII and PSI, was given as follows:

$$\varphi_{Eo} = ET_0/ABS = \varphi_{Po}\cdot\psi_{Eo} = (1 - F_O/F_M)\cdot(1 - V_J)$$

The quantum yield for the reduction of end electron acceptors at the PSI acceptor side: $\varphi_{Ro} = \varphi_{Po}\cdot\psi_{Eo}\cdot\delta_{Ro} = R_{E0}/ABS = \varphi_{Po}\cdot(1 - V_I)$. Since, $\delta_{Ro} = RE_0/ET_0 = (1 - V_I)/(1 - V_J)$. φ_{Ro} expresses the maximum quantum yield that an absorbed photon by PSII transports an electron from water to the final electron acceptors of PSI.

The performance indices PI_{ABS} and PI_{total} express performances potentials for energy conservation at the sequential bifurcations from photons absorbed by PSII to the reduction of intersystem electron acceptors as PI_{ABS} and to the reduction of PSI end acceptors as PI_{total}, respectively. They can be calculated as follows [22]:

$$PI_{ABS} = [\gamma_{RC}/(1 - \gamma_{RC})]\cdot[\varphi_{Po}/(1 - \varphi_{Po})]\cdot[\psi_{Eo}/(1 - \psi_{Eo})]$$

$$\begin{aligned} PI_{total} &= PI_{ABS}\cdot\delta_{Ro}/(1 - \delta_{Ro}) \\ &= [\gamma_{RC}/(1 - \gamma_{RC})]\cdot[\varphi_{Po}/(1 - \varphi_{Po})]\cdot[\psi_{Eo}/(1 - \psi_{Eo}) \\ &\quad \times]\cdot \delta_{Ro}/(1 - \delta_{Ro}) \end{aligned}$$

where γ is the fraction of reaction center chlorophyll of PSII (Chl_{RC}) per total chlorophyll of PSII (Chl_{RC} + $Chl_{Antenna}$), therefore $\gamma_{RC}/(1 - \gamma_{RC}) = Chl_{RC}/Chl_{Antenna} = RC/ABS$. Expressed in experimental fluorescence terms $RC/ABS = RC/TR_0$. $TR_0/ABS = (M_0/V_J).(1 - F_O/F_M)$ where M_0 is the slope at time ~zero of the relative variable fluorescence between F_O and F_M. The maximal slope is $M_0 \equiv (\Delta V/\Delta t)_0$, and where $V = (F_t - F_O)/(F_M - F_O)$.

Acknowledgments

The work was supported by National Natural Science Foundation of China (30671382) and Natural Science Foundation of Guangdong Province (6022863) and NSF of Jiangsu (BK2012764) and China 863 Program (2011AA10A206) and 111 project (B07030). We acknowledge Professor Tom Hsiang (University of Guelph) for his editorial advice.

References

[1] R. Barreto, A. Charudattan, A. Pomella, R. Hanada, Biological control of neotropical aquatic weeds with fungi, Crop Prot. 19 (2000) 697–703.
[2] M.M. Xiang, Y.S. Zeng, R. Liu, S.Q. Chen, J.H. Cai, M.L. You, Host range, conditions for conidium-producing and efficacy in Alligator weed control of *Nimbya alternantherae*, Acta Phytopathol. Sin. 32 (2002) 285–287.
[3] M.M. Xiang, Y.S. Zeng, R. Liu, X.L. Qin, Herbicidal activity of metabolite produced by *Nimbya alternantherae*, a leaf spot pathogen of *Alternanthera philoxeroide*, Chin. J. Biol. Control 18 (2002) 87–89.

[4] Y.P. Zhou, M.M. Xiang, Z.D. Jiang, H.P. Li, W. Sun, H.L. Lin, H.Z. Fan, Separation, purification and structural identification of the phytotoxin from *Nimbya alternantherae*, Chem. J. Chin. Univ. 27 (2006) 1485–1487.
[5] Y. Kimura, M. Nishibe, H. Nakajima, T. Hamasaki, Vulculic acid, a pollen germination inhibitor produced by the fungus, *Penicillium* sp. Agric. Biol. Chem. 55 (1991) 1137–1138.
[6] M.M. Xiang, L.L. Fan, Y.S. Zeng, Y.P. Zhou, Study on the herbicidal activity of vulculic acid from *Nimbya alternantherae*, in: M.H. Julien, R. Sforza, M.C. Bon, H.C. Evans, P.E. Hatcher, H.L. Hinz, B.G. Rector (Eds.), Proceedings of the XII International Symposium on Biological Control of Weeds, CAB International, Wallingford, Oxfordshire, UK, 2008, pp. 349–352.
[7] Y.S. Zeng, M.M. Xiang, Y.P. Xie, The pathogenic mechanism of toxin from *Nimbya alternantherae* to *Alternanthera philoxeroides*, J. Zhongkai Agric. Tech. Univ. 18 (4) (2005) 1–5.
[8] Y.X. Zhang, L.L. Fan, Z.R. Shi, Z.D. Jiang, J.H. Huang, M.M. Xiang, Effects of vulculic acid on the ultra-structure of leaf and root tip tissues of *Alternanthera philoxeroides*, J. Huazhong Agric. Univ. 30 (2011) 84–88.
[9] J. Xiong, G. Jee, S. Subramaniam, Modeling of the D1/D2 proteins and cofactors of the photosystem II reaction center: implications for herbicide and bicarbonate binding, Protein Sci. 5 (1996) 2054–2073.
[10] C. Fedtke, S.O. Duke, Herbicides, in: B. Hock, E.F. Elstner (Eds.), Plant Toxicology, fourth ed., Marcel Dekker, New York, USA, 2004.
[11] S.G. Chen, X.M. Xu, X.B. Dai, C.L. Yang, S. Qiang, Identification of tenuazonic acid as a novel type of natural photosystem II inhibitor binding in $Q_{\overline{B}}$ site of *Chlamydomonas reinhardtii*, Biochim. Biophys. Acta 1767 (2007) 306–318.
[12] S.G. Chen, C.Y. Yin, X.B. Dai, S. Qiang, X.M. Xu, Action of tenuazonic acid, a natural phytotoxin, on photosystem II of spinach, Environ. Exp. Bot. 62 (2008) 279–289.
[13] S.G. Chen, F.Y. Zhou, C.Y. Yin, R.J. Strasser, C.L. Yang, S. Qiang, Application of fast chlorophyll *a* fluorescence kinetics to probe action target of 3-acetyl-5-isopropyltetramic acid, Environ. Exp. Bot. 71 (2011) 269–279.
[14] R.J. Strasser, A. Srivastava, Govindjee, Polyphasic chlorophyll *a* fluorescence transient in plants and cyanobacteria, Photochem. Photobiol. 61 (1995) 32–42.
[15] R.J. Strasser, M. Tsimilli-Michael, A. Srivastava, Analysis of the chlorophyll *a* fluorescence transient, in: G.C. Papageorgiou, Govindjee (Eds.), Chlorophylla Fluorescence: A Signature of Photosynthesis, Springer Press, Netherlands, 2004, pp. 321–362.
[16] P. Pospíßil, H. Dau, Valinomycin sensitivity proves that light-induced thylakoid voltages result in millisecond phase of chlorophyll fluorescence transients, Biochim. Biophys. Acta 1554 (2002) 94–100.
[17] G. Schansker, S.Z. Tóth, R.J. Strasser, Methylviolegen and dibromothymoquinone treatments of pea leaves reveal the role of photosystem I in the Chl *a* fluorescence rise OJIP, Biochim. Biophys. Acta 1706 (2005) 250–261.
[18] A. Kanazawa, D.M. Kramer, In vivo modulation of nonphotochemical exciton quenching (NPQ) by regulation of the chloroplast ATP synthase, Proc. Natl. Acad. Sci. U.S.A. 99 (2002) 12789–12794.
[19] R.J. Strasser, Govindjee, The F_O and the O–J–I–P fluorescence rise in higher plants and algae, in: J.H. Argyroudi-Akoyunoglou (Ed.), Regulation of Chloroplast Biogenesis, Plenum Press, New York USA, 1992, pp. 423–426.
[20] A.J. Strauss, G.H.J. Kruger, R.J. Strasser, P.D.R. Van Heerden, Ranking of dark chilling tolerance in soybean genotypes probed by the chlorophyll *a* fluorescence transient OJIP, Environ. Exp. Bot. 56 (2006) 147–157.
[21] A. Srivastava, F. Juttner, R.J. Strasser, Action of the allelochemical, fischerellin A, on photosystem II, Biochim. Biophys. Acta 1364 (1998) 326–336.
[22] R.J. Strasser, M. Tsimilli-Michael, S. Qiang, V. Goltsev, Simultaneous in vivo recording of prompt and delayed fluorescence and 820-nm reflection changes during drying and after rehydration of the resurrection plant *Haberlea rhodopensis*, Biochim. Biophys. Acta 1797 (2010) 1313–1326.
[23] A. Stirbet, Govindjee, B.J. Strasser, Chlorophyll *a* fluorescence induction in higher plants: modeling and numerical simulation, J. Theor. Biol. 193 (1998) 131–151.
[24] X.G. Zhu, Govindjee, N.R. Baker, Chlorophyll *a* fluorescence induction kinetics in leaves predicted from a model describing each discrete step of excitation energy and electron transfer associated with photosystem II, Planta 223 (2005) 114–133.
[25] P.A. Jursinic, Flash polarographic detection of superoxide production as a means of monitoring electron flow between photosystems I and II, FEBS Lett. 90 (1978) 15–20.
[26] D. Arnon, Copper enzymes in isolated chloroplasts: polyphenoloxidase in *Betavulgaris*, Plant Physiol. 24 (1949) 1–15.
[27] J. Coombs, D.O. Hall, S.P. Long, J.M.O. Scurlock, Techniques in Bioproductivity and Photosynthesis, Science Press, Beijing China, 1986.
[28] Y.Z. Li, J.M. Wei, Experiment Manual of Modern Plant Physiology, Science Press, Beijing, China, 1999.
[29] Z.H. Huang, Experiment Manual of Plant Physiology, Shanghai Science and Technology Press, Shanghai, China, 1985.
[30] J.T. Perchorowicz, D.A. Raynes, R.G. Jensen, Measurement and preservation of the in vivo activation of ribulose-1,5-bisphosphate carboxylase in leaf extracts, Plant Physiol. 69 (1982) 1165–1168.
[31] M.M. Bradford, A rapid and sensitive method for the quantitation of microgram quantities of protein utilizing the principle of protein–dye binding, Anal. Biochem. 72 (1976) 248–254.